

# A Cytology Dataset for Early Detection of Oral Squamous Cell Carcinoma

**Garima Jain**<sup>1,3,\*</sup>, **Sanghamitra Pati**<sup>4</sup>, **Mona Duggal**<sup>3</sup>, **Amit Sethi**<sup>2</sup>, **Abhijeet Patil**<sup>2</sup>, **Gururaj Malekar**<sup>3</sup>, **Nilesh Kowe**<sup>3</sup>, **Jitender Kumar**<sup>3</sup>, **Jatin Kashyap**<sup>3</sup>, **Divyajeet Rout**<sup>3</sup>, **Deepali**<sup>3</sup>, **Hitesh**<sup>3</sup>, **Nishi Halduniya**<sup>3</sup>, **Sharat Kumar**<sup>3</sup>, **Heena Tabassum**<sup>5</sup>, **Rupinder Singh Dhaliwal**<sup>5</sup>, **Sucheta Devi Khurajam**<sup>6</sup>, **Sushma Khurajam**<sup>6</sup>, **Sharmila Laishram**<sup>6</sup>, **Simmi Kharb**<sup>7</sup>, **Sunita Singh**<sup>7</sup>, **K. Swaminadhan**<sup>8</sup>, **Ranjana Solanki**<sup>9</sup>, **Deepika Hemranjani**<sup>9</sup>, **Shashank Nath Singh**<sup>10</sup>, **Uma Handa**<sup>11</sup>, **Manveen Kaur**<sup>11</sup>, **Surinder Singh**<sup>12</sup>, **Shivani Kalhan**<sup>13</sup>, **Rakesh Kumar Gupta**<sup>13</sup>, **Ravi. S**<sup>14</sup>, **D. Pavithra**<sup>15</sup>, **Sunil Kumar Mahto**<sup>16</sup>, **Arvind Kumar**<sup>16</sup>, **Deepali Tirkey**<sup>16</sup>, **Saurav Banerjee**<sup>16</sup>, and **L. Sreelakshmi**<sup>17</sup>

<sup>1</sup>Indian Council of Medical Research-National Institute for Research in Digital Health & Data Science, New Delhi

<sup>2</sup>Department of Electrical Engineering, IIT Bombay

<sup>3</sup>Koita Centre of Digital Health, IIT Bombay

<sup>4</sup>Indian Council of Medical Research, New Delhi

<sup>5</sup>Division of Non Communicable Diseases, Indian Council of Medical Research, New Delhi-110029

<sup>6</sup>Department of Pathology, Regional Institute of Medical Sciences, Imphal

<sup>7</sup>Department of Biochemistry, Pt BD Sharma PGIMS, Rohtak

<sup>8</sup>Institute of Pathology, Madras Medical College, Chennai

<sup>9</sup>Department of Pathology SMS Medical College Jaipur

<sup>10</sup>Department of Otorhinolaryngology SMS Medical College Jaipur

<sup>11</sup>Department of Pathology, Government Medical College and Hospital, Chandigarh

<sup>12</sup>Department of Otorhinolaryngology, Government Medical College and Hospital, Chandigarh

<sup>13</sup>Government Institute of Medical Sciences, Greater Noida

<sup>14</sup>Department of Pathology, Chengalpattu Medical College, Chengalpattu

<sup>15</sup>Department of Pathology, Coimbatore medical College, Civil aerodrome post, Coimbatore

<sup>16</sup>Department of Pathology, RIMS, Ranchi, Jharkhand

<sup>17</sup>Gandhi Medical College, Hyderabad, Telangana

\*garima.jain@gmail.com

## ABSTRACT

Oral squamous cell carcinoma (OSCC) is a major global health burden, particularly in several regions across Asia, Africa, and South America, where it accounts for a significant proportion of cancer cases. Early detection dramatically improves outcomes, with stage I cancers achieving up to 90% survival. However, traditional diagnosis based on histopathology has limited accessibility in low-resource settings because it is invasive, resource-intensive, and reliant on expert pathologists. On the other hand, oral cytology of brush biopsy offers a minimally invasive and lower-cost alternative, provided that the remaining challenges – inter-observer variability and unavailability of expert pathologists – can be addressed using artificial intelligence (AI). Development and validation of robust AI solutions requires access to large, labeled, and multi-source datasets to train high-capacity models that generalize across domain shifts. We introduce the first large and multi-center oral cytology dataset, comprising annotated slides stained with Papanicolaou(PAP) and May-Grünwald-Giemsa(MGG) protocols, collected from ten tertiary medical centers in India. The dataset is labeled and annotated by expert pathologists for cellular anomaly classification and detection, is designed to advance AI-driven diagnostic methods. By filling the gap in publicly available oral cytology datasets, this resource aims to enhance automated detection, reduce diagnostic errors, and improve early OSCC diagnosis in resource-constrained settings, ultimately contributing to reduced mortality and better patient outcomes worldwide.

## Background and Summary

Oral squamous cell carcinoma (OSCC) is a major global public health challenge. It is the most common head and neck malignancy and the sixth most common tumor worldwide<sup>1</sup>. Despite advances in therapies, overall mortality continues to be high and has remained unchanged during the past decades because almost half of OSCC cases are diagnosed in advanced stages

(III or IV), with 5-year survival rates 5-20%.<sup>2</sup> On the contrary, survival rates of stage I cancer are up to 90%. Thus, early diagnosis and referral are the cornerstone for reducing cancer-related mortality.<sup>3,4</sup> Most often the delay is due to the time gap (which is avoidable) between patient's initial contact with a healthcare provider and obtaining a referral for specialist care and treatment.<sup>5</sup> Histopathological analysis of tissue obtained through surgical biopsy is considered the gold standard for diagnosing oral lesions. The absence of trained pathologists at the primary care level and the lack of essential resources for the processing of the biopsy, such as paramedical staff and equipment (e.g., automatic tissue processor), collectively hinder timely diagnosis, particularly in low-income countries.<sup>5,6</sup>

Cytology of brush biopsy is a simpler, safer, and less invasive alternative to histopathology of surgical biopsy, which can be equally reliable for early detection of oral malignancies.<sup>7</sup> In brush biopsy, tissue samples from the oral mucosa are collected for morphological evaluation using a firm brush on the mucosal surface with sufficient pressure to cause pinpoint bleeding to ensure the collection of a full-thickness or transepithelial sample. These cellular samples can be further analyzed using techniques such as microscopy, DNA cytometry, and immunocytochemical assays<sup>8</sup>. Using exfoliative cytology can help reduce the risk of false negative biopsies and eliminate the risk of postbiopsy complications<sup>9</sup>. Oral cytology is recognized as a valuable tool for large-scale screening in high-risk populations.<sup>10</sup>

While oral cytology demonstrates significant potential for identifying dysplastic and cancerous lesions, its clinical utility has been hindered by inconsistent false-positive and false-negative rates. This can be attributed to various factors, including technical expertise for interpretation, variability in technical quality, insufficient cellular content in oral smears, and suboptimal sampling techniques.<sup>9</sup> The technique is also labor-intensive and visual interpretation is subjective, time consuming, and require highly specialized medical expertise. Reading a cytology smear is complex. It involves the visual examination of hundreds of thousands of cells to identify atypical ones across a large area.<sup>11</sup> The European guidelines for quality assurance in cervical cancer screening comments that screening duration is linked to the number of fields of view and slide area viewed; less time per specimen means only part of the collected tissue is seen.<sup>11</sup> Studies on auditing of false negative cytology reports in cervical cancer have shown that errors in initial evaluations were a significant factor in nearly half of the false negative reports. In Poland, an audit revealed that over 50% of slides initially deemed normal during screening were later classified as abnormal.<sup>12</sup>

Manually detecting abnormal areas on oral cytopathological slides is a laborious task and requires extensive training to accurately identify abnormal cells under a microscope.<sup>13</sup> To overcome this challenge of limited number of trained cytologists, often a two-step diagnostic process is implemented in low-resource settings. It involves an initial rough screening by cytotechnologists or junior pathologists who manually identify critical diagnostic areas on a slide with an ink marker. These marked areas are then reviewed more thoroughly by a senior pathologist. Unfortunately, the first-step runs the risk of false negatives.

This analysis highlights the need for improved methods and the development of automated approaches to analyze cytology data that can provide greater precision with fewer false negative, false positive, and providing feedback on unsatisfactory tissue collection. The primary objective of automated cytology screening is to enhance the efficiency of cancer screening programs, reduce cancer-related mortality, and improve overall health outcomes. Automated systems also offer the potential to lower healthcare costs tied to cancer diagnosis and treatment, increasing accessibility in resource-constrained areas.<sup>14</sup>

The case of historical advancements in automated screening systems for cervical cancer can serve as a guide for OSCC. These systems are increasingly integrating digital scanning tools with AI technologies to aid healthcare professionals in cytological evaluations<sup>15</sup>. The traditional workflow typically involves identifying regions of interest (RoI), segmenting cellular structures, and categorizing cells as either precancerous or cancerous. Over time, telemedicine platforms have demonstrated significant benefits in cytology, enabling remote diagnosis of malignancies in the cervix, lungs, breast and thyroid.<sup>10</sup>

Computer-assisted image analysis of cytopathology samples has also been widely studied and implemented in cervical cancer over the last few decades. Automated cytological screening systems, such as PAPNET<sup>16</sup> and AUTOPAP, were developed in the 1990s and use standardization of slide preparation along with image processing and machine learning algorithms to enhance the efficiency and accuracy of cervical cancer screenings by identifying suspicious areas in Pap smears for further review. These systems have improved detection rates, reduced the workload for cytotechnicians, and reduced costs in screening programs, thereby lowering cervical cancer incidence and mortality.<sup>11</sup> Deep learning can improve the diagnostic accuracy even further.

In deep learning, achieving high accuracy often depends on having a large dataset collected from multiple sources with detailed pixel-wise labeling for segmentation or image-level labeling for classification tasks. However, within the biomedical field, the challenge extends beyond merely obtaining the image data. It also involves securing accurate and relevant annotations for these images from medical experts.<sup>17</sup> Multiple public datasets of cervical cytology images are available, for example, CRIC Cervix<sup>18</sup>, Herlev<sup>19</sup>, SIPaKMeD<sup>20</sup>, DCCL<sup>21</sup>.

On the other hand, the paucity of work on automated detection of lesions on oral cytology can be directly linked to the unavailability of large, relevant, and annotated datasets. On the other hand, lung imaging datasets have been readily accessible on dataset distribution platforms, such as Kaggle and grand-challenge.org, since 2016, which has led to an increase

in publications on lung cancer detection. Similar observations about dataset availability influencing research trends have been noted throughout the history of machine learning.<sup>22</sup> Achieving improved generalization of AI in medical imaging requires the assembly of substantially larger datasets while minimizing biases that can arise from opportunistic data collection.<sup>23</sup>

Some of the factors behind the unavailability of oral cytology datasets is common to medical imaging in general, while other challenges are unique to it. Medical imaging data are not only limited in quantity but also in variety, often restricted by geographical and equipment factors. This limitation makes acquiring a diverse dataset challenging. In medical settings, strict patient privacy regulations hinder the sharing of data between institutions, leading to isolated data silos that pose challenges for collaborative research and model training. Also, the process of annotating medical images is intricate and demands the expertise of trained medical professionals who are already overburdened with clinical work, making it both time-consuming and costly. Additionally, oral cytology has typically been neglected in data collection and machine learning primarily because it disproportionately afflicts resource-constrained countries, where chewing tobacco or betel nut is more common and funds for medical research are harder to come by.

With the aim to enable development of reliable AI-based pipelines for cost-effective and accurate detection of OSCC, we introduce the first of its kind large, expertly annotated, and multi-institutional oral cytology dataset of brush biopsies. The dataset covers over 200 patients, two stain types (Pap and MGG), multi-category benign controls and confirmed malignancies, and 10 institutions. We describe the dataset preparation methods and its characteristics next.

**Table 1.** Dataset key statistics

Attribute	Key statistics
Number of Patients	234
Number of WSIs	368
Stain types	PAP – 184, MGG – 184
Age	Range – 18 to 70 years Mean – 44 years Median – 45 years
Gender	Male – 194, Female – 40
Diagnosis	Non Cancerous – 197 (306) Cancerous – 42 (74)
Category	Category I – 162 (244) Category II – 35 (62) Category III – 24 (47) Category IV – 18 (27)
Hospital centers	Maulana Azad Medical College, New Delhi – 59 (105) Sawai Man Singh Medical College, Jaipur – 65 (99) Rajendra Institute of Medical Sciences, Ranchi – 40 (75) Regional Institute of Medical Sciences, Imphal – 19 (29) Government Institute of Medical Sciences, Noida – 16 (20) Tirunelveli Medical College, Tamil Nadu – 16(18) Government Medical College and Hospital, Chandigarh – 8 (10) Pandit Bhagwat Dayal Sharma Post Graduate Institute of Medical Sciences, Rohtak – 7 (8) Coimbatore Medical College, Coimbatore – 3 (3) Gandhi Medical College, Secunderabad – 1 (1)

## Methods

We now describe sample collection, digitization, and annotation methods. Prospective multicentric cohort study was conducted at 10 tertiary medical colleges and associated hospitals in India. Ethical clearance was obtained from all centers and ICMR. The study was carried out between 15<sup>th</sup> May, 2023 and 15<sup>th</sup> September, 2024. The data covers both sexes and a wide age range of the adult population. The summary of the data samples is shown in Table 1.

### Sample collection

Brush cytology was performed by the doctor in charge at the respective multidisciplinary research unit, following standard protocols. The patient's mouth was rinsed with water to remove cellular debris. For patients with lesions, the lesion was visualized under adequate illumination and a toothbrush or oral brush was brushed repeatedly in a single direction over the

entire lesion until pinpoint bleeding was observed. To collect cytology smears from healthy controls, the inner surface of the cheek was scraped along the buccal mucosa. The material obtained was quickly smeared and spread on the middle third of a minimum of two clean, dried glass slides. Each slide was labeled with two unique identifiers. One of the slides was fixed in 95% ethanol for 15 minutes for Papanicolaou staining and the rest of the slides were air dried for MGG staining, according to uniform staining protocols. A requisition form with details of site, clinical characteristics, radiological findings, and related preoperative findings was collected. The slides were rejected if they were unlabeled, mislabeled, separated from their request and without the cytopathological request form duly completed by the treating physician. All papanicolaou and May-Grünwald-Giemsa (MGG) protocol stained slides were independently evaluated by at least two pathology diagnostic experts. Any discrepancy in the assessment was resolved by consensus. Oral brush cytology can be reported in The Papanicolaou grading system and The Bethesda classification system. Standard operating protocols were prepared and shared with all the respective centers to maintain uniformity.

## Digitization

A total of 368 cytopathological slides were digitized using high-resolution 3DHISTECH whole slide scanners with a magnification of 40 $\times$ , ensuring detailed visualization of cellular structures for downstream analysis. Among these, 58 whole slide images (WSIs) were scanned at a spatial resolution of 0.125 microns per pixel ( $\mu\text{m}/\text{pixel}$ ), while the remaining 310 WSIs were acquired at a resolution of 0.24  $\mu\text{m}/\text{pixel}$ . This dual-resolution dataset captures both fine-grained and broader tissue contexts, enhancing the robustness of morphological studies. On an average, the WSIs measured approximately 83,000 pixels in width and 168,000 pixels in height, indicative of the extensive tissue coverage.

## Annotation

The annotation process begins with an expert pathologist identifying viable regions of 2048 $\times$ 2048 pixels each within a WSI, which were carefully selected to represent areas of interest for further analysis. On an average, five such regions are annotated per slide, providing a robust representation of the tissue sample. Following the identification of viable regions, each region undergoes a detailed annotation process for nucleus segmentation, facilitated by QuPath<sup>24</sup>, an open-source software designed for digital pathology. The annotation of viable regions typically requires around five minutes per slide. In contrast, the nucleus segmentation annotation process is more time-intensive, requiring approximately 15 minutes per patch due to the meticulous nature of labeling each nucleus. Each nucleus within the segmented regions is assigned a label ranging from one to four, based on established cytological criteria. This rigorous annotation process ensures high-quality data for downstream analyses and provides a reliable foundation for further computational studies. Digitization and annotation process is shown in Figure 1 and annotated dataset is summarized in Table 2.

## Data Records

The dataset, containing annotated whole slide image (WSIs), patches with nucleus annotations, is publicly available on various platforms, such as [Kaggle](#), and [Google Drive](#). Given the large size of WSIs, totaling approximately 700GB across 368 slides in MRXS format, hosting on Google Drive ensures easier access for researchers. In addition to the WSIs, the dataset includes a CSV file with patient and slide-level metadata, capturing clinical details such as smoking history, family history, and diagnostic findings. For more focused analysis, 858 high-resolution image patches (2048 $\times$ 2048 pixels) have been extracted from 168 WSIs, selected based on the presence of viable cells. These patches are accompanied by detailed nucleus annotations provided in QuPath-compatible GeoJSON format, enabling precise cell segmentation. To streamline processing and integration into machine learning pipelines, sample code is available on [GitHub](#) to convert the GeoJSON nucleus annotations into binary masks or instance segmentation masks, supporting both semantic segmentation and instance-level analysis. The comprehensive organization and multi-platform availability of this dataset aim to facilitate collaborative research and reproducibility across the community.

**Table 2.** Model performance on the validation dataset for binary instance segmentation. The table reports overall segmentation metrics as well as class-wise performance across four categories. Notably, categories 3 and 4 exhibit lower scores, likely due to class imbalance and their under-representation in the training data compared to categories 1 and 2.

Method	AJI	DQ	SQ	PQ	$F_d$	$F_I$	$F_{II}$	$F_{III}$	$F_{IV}$
UNet <sup>25</sup>	0.740	0.729	0.694	0.514	0.811	0.452	0.164	0.084	0.119
UNet++ <sup>26</sup>	0.741	0.732	0.702	0.516	0.823	0.518	0.218	0.112	0.132
HoverNet <sup>27</sup>	0.752	0.758	0.743	0.542	0.835	0.553	0.228	0.164	0.192
StarDist <sup>28</sup>	0.741	0.754	0.728	0.528	0.845	0.548	0.239	0.169	0.175

**Table 3.** Summary statistics of the dataset used, showing the number of whole slide images (WSIs), extracted patches, and annotated nuclei across four categories (I–IV).

	<b>I</b>	<b>II</b>	<b>III</b>	<b>IV</b>	<b>Total</b>
# of WSIs	97	14	26	25	162
# of patches	523	92	140	112	867
# of nuclei	19888	6175	6022	7161	39246

## Technical Validation

Baseline segmentation models were developed using the annotated dataset. For each experimental run, data from six centers were used for training, two centers for validation, and two centers for testing. This center-based splitting strategy ensures robust evaluation by testing the models on data from centers unseen during training. The baseline models include UNet<sup>25</sup>, UNet++<sup>26</sup>, StarDist<sup>28</sup>, and HoverNet<sup>27</sup>, each of which was trained to perform nucleus segmentation on the dataset. The training codes for these models are publicly available on GitHub, allowing reproducibility and further experimentation. Model performance was evaluated using three key metrics: dice score, aggregated Jaccard index, and panoptic quality. These metrics provide comprehensive insights into the segmentation accuracy, overlap quality, and instance-level performance of the models. A detailed comparison of the results for each model is summarized in Table 2. This baseline provides a foundation for future research and improvements for the segmentation tasks. The overall procedure of the dataset preparation and validation is depicted in Figure 1.

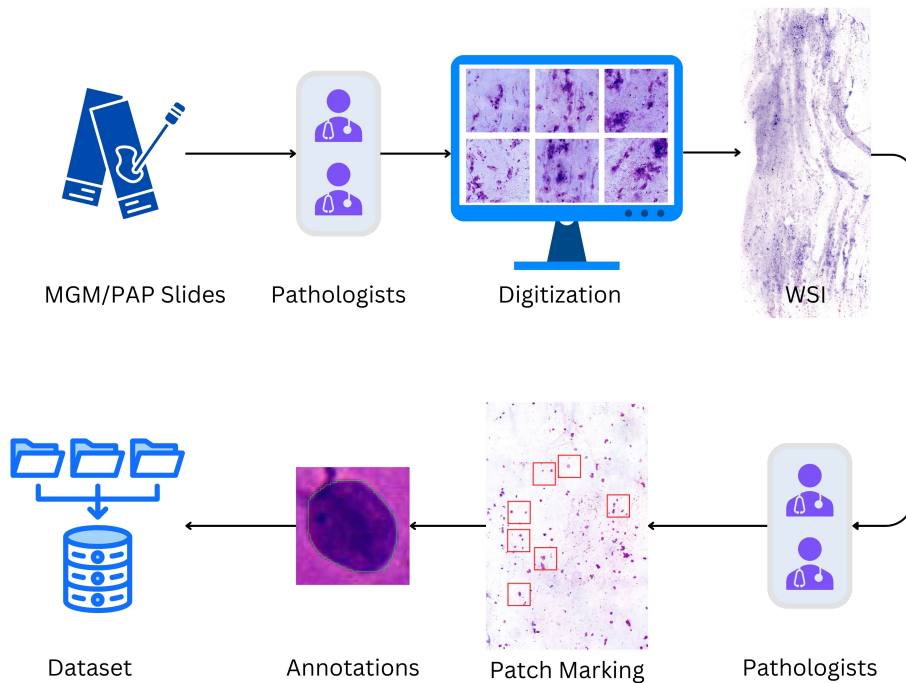


**Figure 1.** The overall procedure for dataset creation for training the AI segmentation model.

## Code Availability

Codes to train segmentation models using images and GeoJson annotations is available publicly on [GitHub](#).

## References

1. Tan, Y. *et al.* Oral squamous cell carcinomas: state of the field and emerging directions. *Int. journal oral science* **15**, 44 (2023).

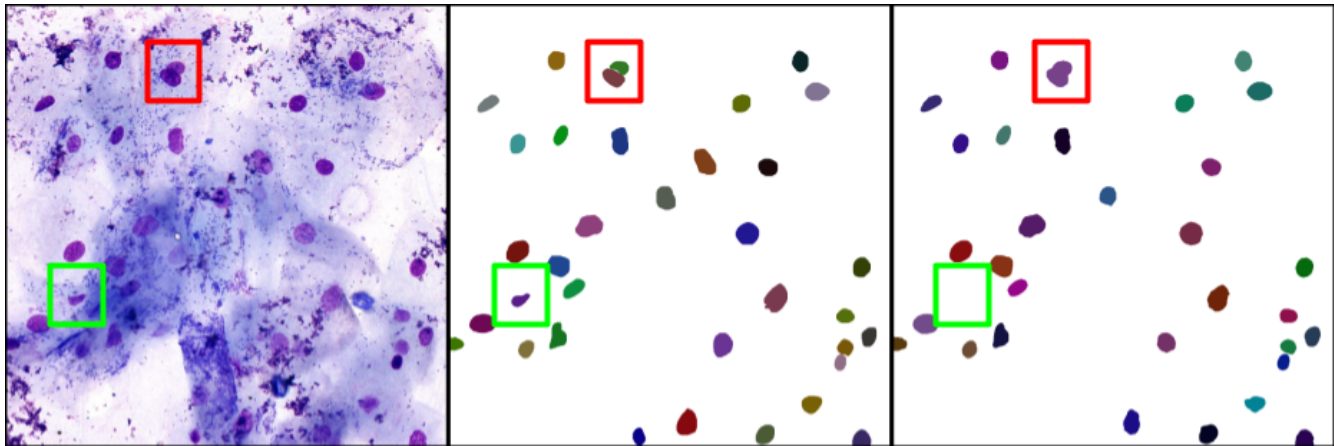


**Figure 2.** From left to right: input histological image, ground truth annotation, and prediction output from the U-Net++<sup>26</sup> model. Regions outlined in red and green highlight areas where the model is likely to err. The red box denotes adjacent nuclei in close proximity, posing a challenge for accurate instance separation. The green box indicates a nucleus with faint cytoplasmic boundaries and an irregular shape, which the model fails to detect.

2. Ramachandran, S. Oral cancer: Recent breakthroughs in pathology and therapeutic approaches. *Oral Oncol. Reports* **12**, 100678 (2024).
3. Jain, G. *et al.* Peripheral blood involvement in angioimmunoblastic t-cell lymphoma: A case report and review of the literature. *Am. J. Blood Res.* **10**, 257 (2020).
4. Jain, G. *et al.* Next generation sequencing guided treatment modulation and prognosis in acute myeloid leukemia: Case vignettes. *Am. J. Blood Res.* **10**, 134 (2020).
5. Swaminathan, D., George, N. A., Thomas, S. & Iype, E. M. Factors associated with delay in diagnosis of oral cancers. *Cancer Treat. Res. Commun.* **40**, 100831 (2024).
6. Jain, G. *et al.* Esophageal squamous cell carcinoma metastatic to umbilicus: a case report with review of literature. *J. Gastrointest. Cancer* **50**, 1018–1021 (2019).
7. Premalignant conditions of the oral cavity: Overview, epidemiology, risk factors and pathophysiology (2023).
8. Driemel, O. *et al.* Diagnosis of oral squamous cell carcinoma and its precursor lesions. *JDDG: J. der Deutschen Dermatol. Gesellschaft* **5**, 1095–1100 (2007).
9. Jairajpuri, Z. S., Rana, S., Hajela, A. & Jetley, S. Toward early diagnosis of oral cancer: Diagnostic utility of cytomorphological features, a pilot study. *Natl. J. Maxillofac. Surg.* **10**, 20–26 (2019).
10. Sunny, S. *et al.* A smart tele-cytology point-of-care platform for oral cancer screening. *PLOS ONE* **14**, e0224885 (2019).
11. Arbyn M., A. A. & J., J. European guidelines for quality assurance in cervical cancer screening (2008).
12. Macios, A., Komerska, K. & Nowakowski, A. Reasons for truly negative cytology reports preceding the diagnoses of invasive cervical cancer—results of a false-negative cytology audit in polish cervical cancer screening programme. *Cancer Med.* **12**, 13800–13810 (2023).
13. Sukegawa, S. e. a. Effective deep learning for oral exfoliative cytology classification. *Sci. Rep.* **12**, 13281 (2022).
14. Sekhar, A. *et al.* Her2 and fish status prediction in breast biopsy h&e-stained images using deep learning. In *2024 IEEE 24th International Conference on Bioinformatics and Bioengineering (BIBE)*, 1–8 (IEEE, 2024).
15. Jiang, P. e. a. A systematic review of deep learning-based cervical cytology screening: from cell identification to whole slide image analysis. *Artif. Intell. Rev.* **56**, 2687–2758 (2023).
16. Cenci, M., Nagar, C. & Vecchione, A. Papnet-assisted primary screening of conventional cervical smears. *Anticancer. research* **20**, 3887–3889 (2000).
17. Deng, R. e. a. Cross-scale attention guided multi-instance learning for crohn's disease diagnosis with pathological images. In *International Workshop on Multiscale Multimodal Medical Imaging*, 24–33 (Springer, 2022).

18. Rezende, M. T. *et al.* Cric searchable image database as a public platform for conventional pap smear cytology data. *Sci. data* **8**, 151 (2021).
19. Marinakis, Y., Dounias, G. & Jantzen, J. Pap smear diagnosis using a hybrid intelligent scheme focusing on genetic algorithm based feature selection and nearest neighbor classification. *Comput. Biol. Medicine* **39**, 69–78 (2009).
20. Plissiti, M. E. *et al.* Sipakmed: A new dataset for feature and image based classification of normal and pathological cervical cells in pap smear images. In *2018 25th IEEE International Conference on Image Processing (ICIP)*, 3144–3148, DOI: [10.1109/ICIP.2018.8451588](https://doi.org/10.1109/ICIP.2018.8451588) (2018).
21. Che, S., Liu, D., Zhang, C., Tu, D. & Luo, P. Dccl: A fundamental dataset of cervical cancer cytological screen using deep learning technology. *J Cytol Tissue Biol* **6**, 024 (2019).
22. Kohli M. D., S. R. M. & R., G. J. Medical image data and datasets in the era of machine learning—whitepaper from the 2016 c-mimi meeting dataset session. *J. Digit. Imaging* **30**, 392–399 (2017).
23. Sood, A., Mishra, D., Yadav, R., Bhatt, K. & Priya, H. The application of the bethesda system for reporting cervical cytology to oral cytology: An institutional study. *Clin. Cancer Investigig. J.* **11**, 25–32 (2022).
24. Bankhead, P. *et al.* Qupath: Open source software for digital pathology image analysis. *Sci. reports* **7**, 1–7 (2017).
25. Ronneberger, O., Fischer, P. & Brox, T. U-net: Convolutional networks for biomedical image segmentation. In *Medical image computing and computer-assisted intervention—MICCAI 2015: 18th international conference, Munich, Germany, October 5-9, 2015, proceedings, part III* 18, 234–241 (Springer, 2015).
26. Zhou, Z., Rahman Siddiquee, M. M., Tajbakhsh, N. & Liang, J. Unet++: A nested u-net architecture for medical image segmentation. In *Deep learning in medical image analysis and multimodal learning for clinical decision support: 4th international workshop, DLMIA 2018, and 8th international workshop, ML-CDS 2018, held in conjunction with MICCAI 2018, Granada, Spain, September 20, 2018, proceedings* 4, 3–11 (Springer, 2018).
27. Graham, S. *et al.* Hover-net: Simultaneous segmentation and classification of nuclei in multi-tissue histology images. *Med. image analysis* **58**, 101563 (2019).
28. Stevens, M. *et al.* Stardist image segmentation improves circulating tumor cell detection. *Cancers* **14**, 2916 (2022).

## Acknowledgments

## Author contributions

## Competing interests

The authors declare no competing interests.

## Additional information